FLOW DYNAMICS IN A SWIRLING JET COMBUSTOR

F.F. Grinstein, [a] T.R. Young,[a] G. Li, [b] E.J. Gutmark,[b] G. Hsiao, [c] and H.C. Mongia[c]

[a] Naval Research Laboratory, Washington DC 20375-5344, USA, grinstein@lcp.nrl.navy.mil

[b] Engineering Research Center, University of Cincinnati, Cincinnati, OH 45221, USA

[c] General Electric Aircraft Engine Company, Cincinnati, OH 45215, USA

ABSTRACT

A hybrid simulation approach is used to investigate the flow patterns in an axisymmetric swirl combustor configuration. Effective inlet boundary conditions are based on velocity data from RANS or actual laboratory measurements at the outlet of a fuel-injector nozzle, and LES is used to study the unsteady non-reactive flow dynamics within the combustor. Case studies ranging from single-swirler to more complex multi-swirler nozzles are presented to emphasize the importance of initial inlet conditions on the behavior of the swirling flow entering a sudden expansion area, including swirl and radial numbers, inlet length, and characteristic velocity profiles.

INTRODUCTION

The present studies are devoted to the axisymmetric swirl combustor configuration shown schematically in Fig.1. It involves a primary fuel nozzle, within which air is passed through a multi-swirler arrangement to mix and atomize the fuel. Coupling swirling flow motion with sudden expansion to the full combustor diameter provides an effective way of enhancing the fuel-air mixing and stabilizing combustion. Because of performance requirements on the design of gas turbine engines, there is considerable interest in identifying optimal swirl and geometrical conditions to achieve specific practical goals in actual flight regimes, such as reduced emissions, improved efficiency and stability.

Numerical simulations of compressible flows developing in both space and time with precise control of initial and boundary conditions are ideally suited in the quest to recognize and understand the local and global nature of the flow instabilities driving the combustor performance – which are the main focus of the work. Numerical experiments can be used to isolate suspected fundamental mechanisms from others which might confuse issues, and extensive space/time diagnostics available based on the simulation database can be exploited to develop analytical and conceptual basis for improved modeling of the turbulent flame.

In simulations for engineering problems involving turbulent combustion, a Reynolds-Averaged Navier-Stokes (RANS) description of the flow [1] and simplistic combustion models (e.g.,[2]) are typically combined. This involves simulating only the mean flow field features and modeling the effects of the entire range of turbulent scales. The restricted information provided by this approach regarding the fluid dynamics, combustion and their different interactions, precludes adequate prediction of the important phenomena required to achieve effective control of the combustion processes, such as combustion-induced flow instabilities, cycle-to-cycle variations, and combustion oscillations associated with unsteady vortex dynamics.

Large Eddy Simulations (LES) can provide a promising alternative to RANS in full-scale three-dimensional combustor configurations (e.g.,[3,4]). LES is based on the expectation that the physically meaningful scales of turbulence can be split into two groups: one consisting of the resolved geometry and regime specific scales, and the other associated with the unresolved smallest eddies in the flow, for which the presumed more-universal dynamics is represented with subgrid scale (SGS) closure models. Although LES is capable of simulating flow features which cannot be handled with RANS – such as significant flow unsteadiness and strong vortex-acoustic couplings, the added advantage comes at the expense of computational cost, since LES is typically an order of magnitude more expensive than RANS. As a consequence, hybrid simulation approaches restricting the use of LES to flow regions where crucially needed and using RANS otherwise, are thought to be unavoidable for practical flow configurations (e.g.,[5]).

The hybrid simulation approach used here for the swirl combustor configuration in Fig.1, involves effective boundary conditions emulating the fuel nozzle, and LES to study the flow within the combustor. Case studies ranging from single-swirler to more complex multi-swirler nozzles were investigated. The inlet boundary conditions used to initialize the combustor flow, involve velocity and turbulent intensities based on data from RANS or actual laboratory measurements at the outlet of the fuel-injector nozzle. The paper is restricted to non-reacting combustor flow studies. Ongoing research of reacting flows addressing the interaction between combustion and flow dynamics will be reported separately.

NUMERICAL SIMULATION MODEL

Simulation of turbulent reacting flows encompasses dealing with a broad range of length and time scales. The largest scales of turbulent flows are related to the specific geometry and regime considered, and the smallest scales are associated with the dissipation of turbulent energy through viscosity. In conventional

LES [6], the governing equations are low-pass filtered to remove the dynamics of the smallest eddies, the effects of which are represented by explicit subgrid scale (SGS) closure models. The Monotonically integrated LES (MILES) approach used here provides a promising practical alternative to conventional LES for inhomogeneous, high-Re flows [4,7-9]. Because of the tensorial (anisotropic) nature of the MILES implicit SGS model [8], the MILES framework is expected to be an effective alternative to conventional SGS models when seeking improved LES for inhomogeneous turbulent flows, and particularly so, for combustion problems involving flames of different character for which a unified SGS modeling approach is clearly desirable.

The 3D MILES model involves structured grids, and solves the time-dependent compressible flow conservation equations for total mass, energy, momentum, and species concentrations with appropriate boundary conditions and an ideal gas equation of state. The explicit finite-difference numerical method [10] is based on splitting integrations for convection and other local processes (e.g., multi-species molecular viscosity, mass diffusion, thermal conduction, and finite-rate global chemistry), and coupling them using a timestep splitting approach. Spatial integrations use a fourth-order, one-dimensional Flux-Corrected Transport algorithm at the convection stage, and three-dimensional central differences for the other modeled physical processes; time integrations are performed using a second-order predictor-corrector scheme.

Inlet swirl inflow conditions are discussed below. The outflow boundary conditions at the combustor outlet involve advection of all flow and species variables with Uc, where the instantaneous mean streamwise outlet boundary velocity Uc, is periodically renormalized to ensure that the time-averaged mass-flux coincides with that at the inlet. Two types of outlets are considered (Fig.1). Adiabatic no-slip boundary conditions are imposed at the combustor walls. Additional inflow/outflow numerical boundary conditions required for closure of the discretized equations are chosen based on characteristic analysis as in previous jet simulation studies (e.g.,[4]). Resolution tests in selected cases involved additional runs on finer (126×306×126) and coarser (56×136×56) grids.

The complex flow in the multi-swirler fuel injector nozzle discussed below was simulated using a RANS approach. Due to the complex geometry involved, an unstructured hexahedral mesh created using the ICEM grid generator was used. The RANS results were obtained using the General Electric Aircraft Engine Company (GEAE) Advanced Combustion Code (ACC) on 500,000 hexahedral elements. The calculations were performed using the second-order accurate QUICK discretization scheme. Two turbulence models, including standard k-ε model and cubic k-ε model, were exercised to predict the swirler exit flowfield.

SWIRL INITIAL CONDITIONS

Swirling flow is introduced in practical combustor configurations by appropriately forcing tangential or azimuthal velocity components (e.g., introduced through guide vanes, tangential entry swirlers, or a rotating honeycomb). Initial swirl conditions of various degrees of complexity were considered here to initialize the simulations at the inlet. This included: 1) idealized inflow boundary conditions involving a top-hat profile for the axial velocity U(r), zero radial velocity, and a tangential velocity profile W(r) from RANS of swirling turbulent pipe flows [11]; 2) velocity profiles based on experimental data from a single-swirler practical (LM-6000) combustor configuration [3]; 3) velocity profiles based on RANS or laboratory (PIV or LDV) studies of the flow of a multi-swirler fuel injector. Random velocity fluctuations emulating the RANS turbulent kinetic energy or laboratory measured turbulence intensities are superimposed to the selected mean velocity profiles.

The combustor flows investigated here were characterized by peak inlet free-stream Mach numbers between 0.05–0.3, and STP conditions. Swirl number $\mathcal{S}$ and radial number $\mathcal{R}$ defined by

$$\mathcal{S} = \left[\int_o^{R_o} \rho u w_{\tan} r^2 dr\right] / \left[R_o \int_o^{R_o} \rho u^2 r dr\right],$$

$$\mathcal{R} = \left[\int_o^{R_o} \rho u v_{rad} r dr\right] / \left[\int_o^{R_o} \rho u^2 r dr\right],$$

varying typically between 0–0.75, and between 0–0.5, respectively, were considered, where the inlet radius R_o was chosen to be half of the combustor radius R (Fig.1). Other than passive excitation due to the swirl, the flow was unforced and allowed to naturally develop its unsteadiness.

Turbulent Pipe Flow

This case involved the simplest swirl initial conditions. Inflow boundary conditions at the inlet used a top-hat profile for the axial velocity, zero radial velocity, and a swirl tangential velocity profile based on the RANS study of swirling turbulent pipe flows associated with various body force distributions from [11]. The profile corresponding to a constant body force was used in the present simulations.

LM-6000 Combustor

This device is being developed as operational hardware by GEAE for gas turbine applications and used to test computational modeling capabilities in lean premixed turbulent combustion regimes (see [3] and references therein). Actual laboratory measured nozzle-outlet swirl velocity profiles used to initialize the LES in [3] are compared in Fig.2 for $\mathcal{S}$=0.56 with those of the turbulent pipe flow case – for which the

axial velocity profile is steeper and the tangential velocity peaks closer to (rather than away from) the combustor axis. Radial velocities are identically zero for the pipe flow case, and finite but very small (i.e., R=0.012) for the LM-6000 case.

Multi-Swirl Fuel Injector

A model gas turbine spray combustor based on GEAE and BFGoodrich Aerospace design was used in the experimental and RANS computational work. The combustor features multiple independent fuel supply lines for efficient fuel distribution and multiple air inlets to obtain co- and counter rotating swirling air streams (Fig. 3). The entire combustion air is supplied through the mixer/fuel injector which is located at the combustor dome. The mixer includes three air passages equipped with swirlers lead into the combustion chamber. The two central coaxial passages feature axial swirlers while the external air passage has radial swirling vanes. Air blast fuel atomizers are distributed between the second and third annuli. Fuel is injected into the inner and outer annuli for efficient mixing. A conventional pressure atomized pilot is located in the central passage. This design is typical to industrial dry low emissions combustors.

The location of the fuel injector relative to the sudden expansion at the entrance to the combustion chamber can be varied. The length and exit nozzle of the combustor is variable to allow change in the acoustical boundary conditions, thus enabling excitation of various instability modes. The combustor is retrofitted with quartz windows to allow optical access for Particle Imaging Velocimetry (PIV), Laser Doppler Velocimeter (LDV) and Phase Doppler Particle Analyzer (PDPA) for droplet size and velocity measurements.

A stereoscopic Particle Imaging Velocimetry (PIV) system was used to map the flow field exiting the fuel injector. The three mean and turbulenrt velocity components were measured simultaneously. Two-component PDPA system was used to map the flow field at the exit from the fuel injector and obtain time resolved data as well as measure the dispersion pattern of the simulated injected fuel.

Several studies [12-14] have shown the effect of the combustor inlet conditions on the predicted flame structure, liner temperature, and emissions. These boundary conditions include the axial, tangential and radial velocities, the turbulent kinetic energy and associated length scale. To characterize the flowfield at the exit of the Triple Annular Research Swirler (TARS), two approaches were adopted. First, the advanced diagnosis techniques, including PIV and LDV (discussed above), were used to measure the flowfield distribution at the exit of the swirler. The data collected is used for inlet boundary conditions for the LES and database for numerical model validation. Secondly, a RANS model was used to study mixing and turbulence parameters in the TARS swirler. To eliminate uncertainty on inlet boundary condition specification, the flow domain was extended to the upstream of the swirler vanes. Since the TARS swirler features vane-number 4 for inner, 8 for middle, and 8 for the outer swirler, a 90° pie-sector suffices for the numerical analysis. The operating condition is set to be 1 atm, room temperature (300K), and 4% pressure drop across the TARS swirler.

Typical nozzle conditions investigated are indicated in Table I, where angles α, β, and γ – corresponding to the central, intermediate and external (radial) swirlers, respectively – are used to characterize specific multi-swirler geometries, and S and R are evaluated based on integration of circumferentially- and time-averaged velocity data at the nozzle outlet. Cases I and II are associated with laboratory (PIV) and computational (RANS) studies of the nozzle, respectively. Corresponding radial profiles of the axial, tangential and radial velocities are shown in Fig.4. Compared to the single-swirler profiles, TARS velocity profiles involve much more complex structure, the more noticeable aspect being the annular axial TARS velocities with a characteristic well around the axis – as opposed to the simpler top-hat velocities in Fig.2.

Table I

	Case I	Case II
α	30°	45°
β	30°	45°
γ	45°	30°
S	0.06	0.55
R	0.08	0.48

RESULTS AND DISCUSSION

Single-Swirler Nozzle

Sample results from studies on the combustor of Fig.1 using the turbulent pipe flow inlet conditions are shown in Figs.5-6. The case studies involve S=0.25–0.75, Uo=100m/s, and inlet lengths l/R=0.4–1. For the Reynolds numbers involved here – Re > 300,000, based on mean inlet axial velocity and diameter – vortex breakdown is likely expected to occur for most of the larger values of S considered (e.g.,[15]). The flow is driven by the strong interaction between swirling shear-layer instabilities, on the one side, and flow instabilities driven by the geometry and acoustics of the combustion chamber, on the other. Swirl of sufficient strength produces adverse pressure gradient which can promote flow reversal or vortex breakdown.

The flow pattern associated with the resulting recirculation regions near the jet nozzle axis is similar to the wake flow behind a circular bluff-body; the associated flow instability in the inlet is predominantly helical and resembles a wake flow instability. The second major flow instability is that

introduced by the sudden expansion into the combustion chamber which exhibits features of an annular jet. Interactions between the latter two complex instability modes are directly affected by the swirl magnitude and the relative length of the inlet. Vortex breakdown is observed already for S=0.25, with its occurrence location moving upstream as S increases (Fig.5). Helical structures are dominant in the center recirculation zone as long as they are not initiated inside the inlet pipe. Once vortex breakdown enters deep into the inlet pipe (S=0.75) its structure becomes turbulent and the modes are not easily identifiable. Axisymmetric structure imposed by the sudden expansion is dominant with the shorter inlet length of l/R=0.4 (Fig.6). The longer inlet case is characterized by helical structures caused by vortex breakdown.

Figure 7 further examines the sensitivity of the combustor flow dynamics to the actual choice of initial conditions. The figure now involves contrasting the results of initializing the simulations with the turbulent-pipe or LM-6000 swirling conditions, and otherwise identical initial conditions (S=*0.56,* Uo=100m/s). The flow visualizations depict the significant effects on the combustor vortex dynamics of changing the specifics of the velocity profiles used to initialize the LES, with noticeably more-axisymmetric features observed in the flow features for the LM-6000 case. By design, the swirling pipe flow and LM-6000 swirler cases have similar swirl and radial numbers. The main differences are in the location of the peak tangential velocity component (closer to the axis in the pipe-flow case, and shifted towards the circumference in the LM-6000), and in the more moderate radial gradient of the axial velocity in the LM-6000 swirler. The vortex breakdown appears to be completely eliminated with the LM-6000 swirler, in which case the flow is dominated by the axisymmetric zone at the sudden expansion.

Multi-Swirler Nozzle

Figure 8 exemplifies the velocity distributions at the injector nozzle outlet based on time-averaged PIV data (Fig.8a) and RANS data (Fig.8b), indicating the presence of significant azimuthal inhomogeneities. This suggests that detailed plane (and possibly large-scale unsteady) distributions should be used to initialize the more complex multi-swirler combustor simulations at the inlet – an approach which is now pursued in the ongoing studies. Figure 9 shows distributions of the turbulence kinetic energy from the RANS studies. Strong turbulence is generated when two separate swirling streams meet due to large shear stress and secondary flow effects are clearly noted in the exit of the swirler plane (Fig.8b). The flow field feaures obtained from the PIV and RANS analysis are extracted and serve as inlet condition to simulate the combustor using LES. Figure 10 compares instantaneous flow visualizations from simulations initialized with the circumferentially-averaged profiles associated with these cases (Table I). Again, the flow dynamics is found to be very sensitive to actual initial conditions, e.g., the flow is dominated by axisymmetric features in Case II, for which S and R are very low. Similar differences to those in Fig.7 are observed when Case I and Case II with TARS are compared in Fig. 10. Vortex breakdown does not occur in Case I due to the very low swirl and radial numbers. The high axial component at the circumference prevents strong recirculation at the sudden expansion. Case II with comparable S and pattern of tangential velocity to that of the pipe-flow case in Fig.7 exhibits similar pattern of helical vortex breakdown structure.

Final Remarks

The aforementioned behavior of the various swirlers emphasizes the importance of several parameters on the behavior of the swirling flow entering a sudden expansion area, namely, swirl and radial numbers, inlet length, and specific velocity profiles of the axial, radial and tangential components. In the case of a multi-swirler, the circumferential distribution of the mean and turbulent velocity components is not axisymmetric, and this may have an additional effect on the flow evolution. A systematic study of the interaction between these various parameters and their role in promoting the transition to turbulence is further discussed in the presentation. Relevant issues of supergrid and subgrid modeling are also addressed in this context.

This work was performed with support from the ONR Mechanics and Energy Conversion Division,, with support from ONR through NRL and from the DoD HPC-MP program at NRL and ERDC.

References

[1] Bray, K.N.C. , *26th Int. Symp. on Comb.*, The Combustion Institute, Pittsburgh, (1996), pp.1-26.

[2] Bray, K.N.C. and Libby, P.A., in *Turbulent Reacting Flows*, Eds. Libby, P.A. and Williams, F.A., Academic Press, London (1994), pp.115-152.

[3] Kim, W-W. Menon, , S., and Mongia, H.C. , *Combust.Sci. and Tech.*, **143**, 25 (1999).

[4] Fureby, C. , Kailasanath, K., and Grinstein, F.F., AIAA Paper 2000-0863 (January 2000).

[5] Spalart, P.R. , Jou, W.H., Strelets, M. and Allmaras, S.R., in *Advances in DNS/LES, First AFOSR International Conference in DNS/LES*, Greyden Press, Columbus,1997.

[6] Galperin, B. and Orszag, S.A., *Large Eddy Simulation of Complex Engineering and Geophysical Flows*, CUP, Cambridge (1993).

[7] Boris, J.P., Grinstein, F.F., Oran, E.S. & Kolbe, R.L., Fluid Dyn. Res, **10**,199 (1992).

[8] Fureby, C. & Grinstein, F.F., *AIAA. J,* **37,** 544 (1999).

[9] Fureby, C. & Grinstein, F.F., AIAA Paper 2000-2307 (2000), submitted to *J. Comp. Phys.*

[10] Grinstein, F.F. and Kailasanath, K.K, *Comb. & Flame*, **100**, 2 (1994); **101**, 192 (1995).
[11] Pierce, C.D. & Moin, P., *AIAA J.*, **36**, 1325 (1998).
[12] Hura, H.S., Joshi, N.D., Mongia, H.C., Tonouchi, J., ASME Paper No. 98-GT-444 (1998).
[13] Danis, A. M., Pritchard, B.A., and Mongia, H.C., ASME Paper 96-GT-86 (1996).
[14] Danis, A. M., Burrus, D. L., and Mongia, H. C., *J. Eng. Gas Turbines Power*, **119**, 535 (1997).
[15] Dellenback, P.A. , Metzger, D.E., and Neitzel, G.P. , *AIAA. J*, **26,** 669 (1988).

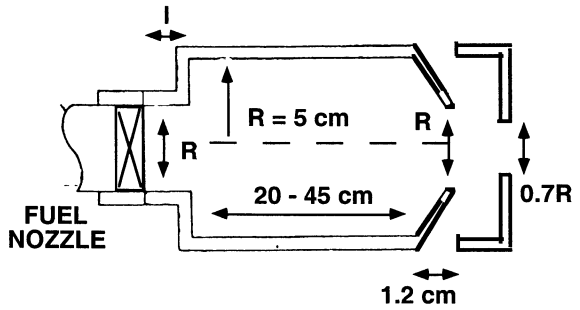

Figure 1. Axisymmetric swirl combustor (the two different outlets used are indicated on the right).

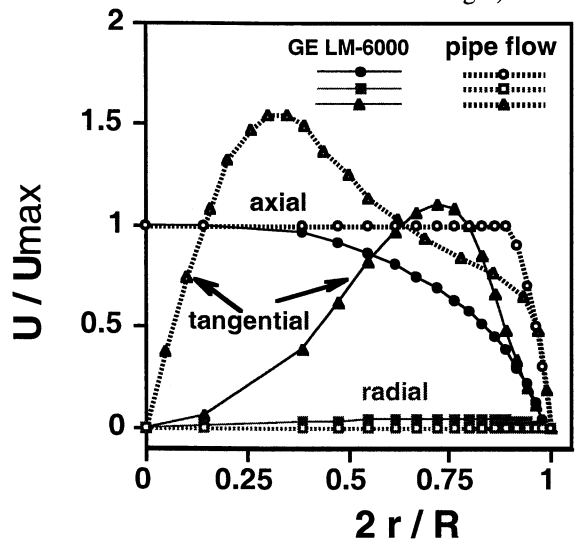

Figure 2. Single-swirler velocity profiles.

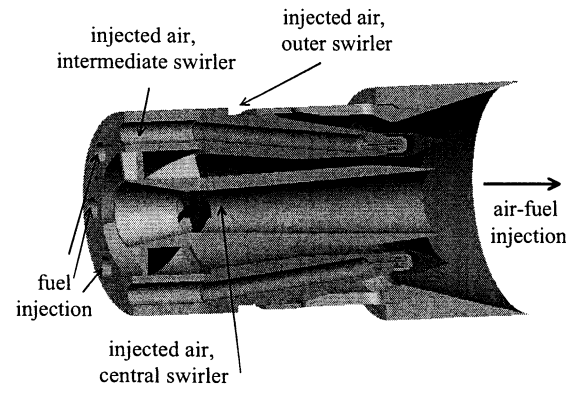

Figure 3. Multi-swirl fuel injector (TARS).

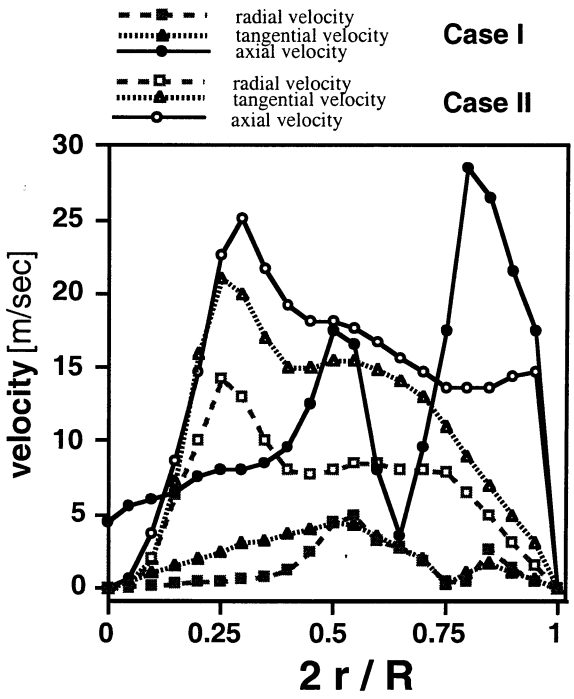

Figure 4. Circumferentially- and time-averaged velocity profiles at the TARS outlet plane.

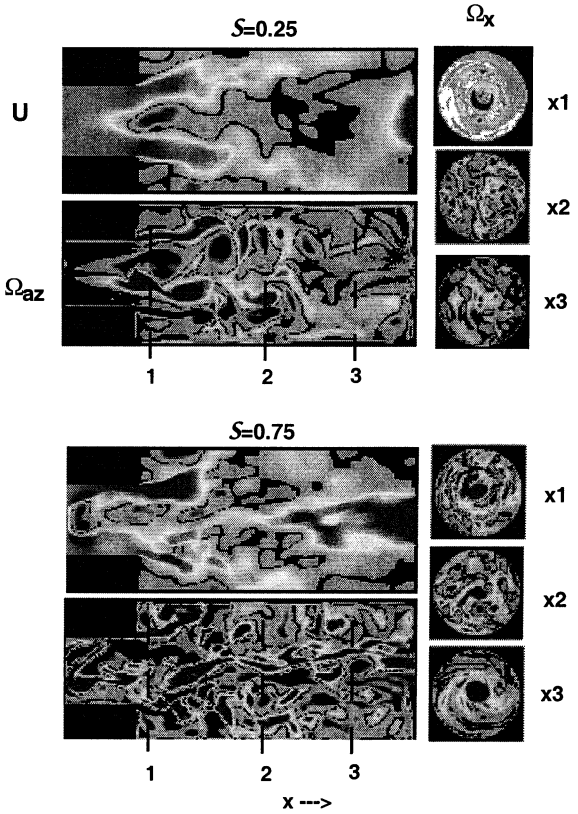

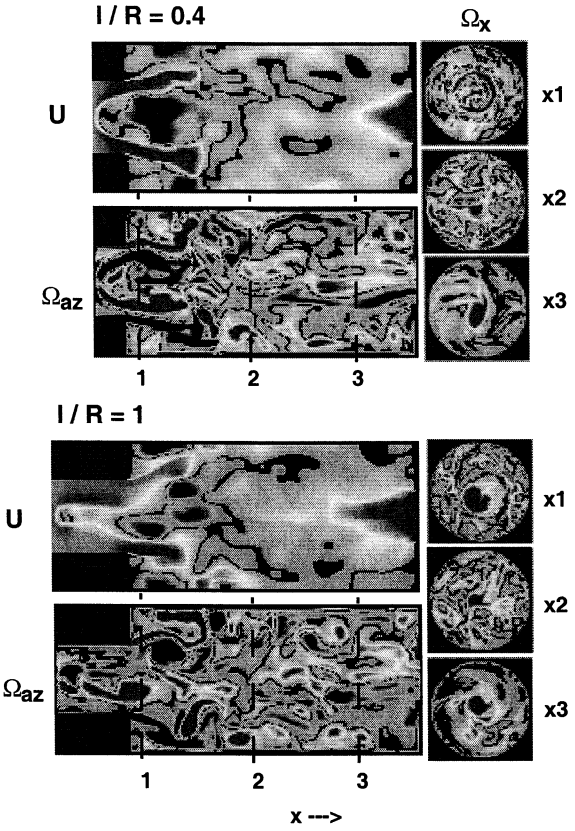

Figure 6. Effects of inlet length for S=0.5.

Figure 7. Effects of initial velocity profiles; LM-6000 (top), turbulent pipe flow (bottom).

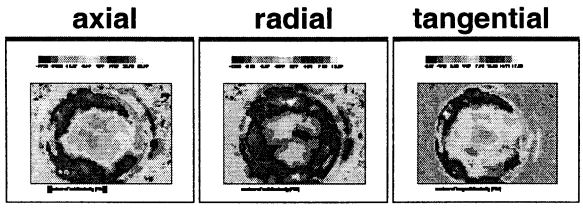

Figure 8a. Velocity at TARS outlet (Case I).

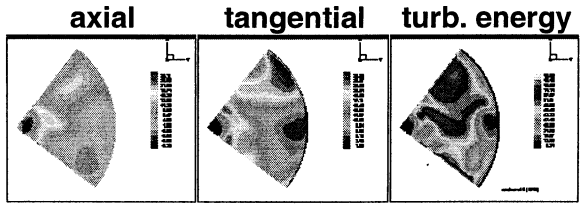

Figure 8b. Distributions at TARS outlet (Case II).

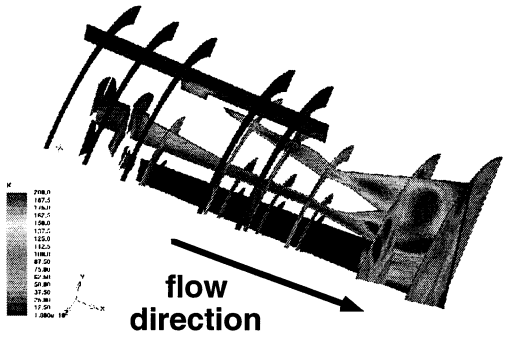

Figure 9. Turbulent kinetic energy (TARS, Case II).

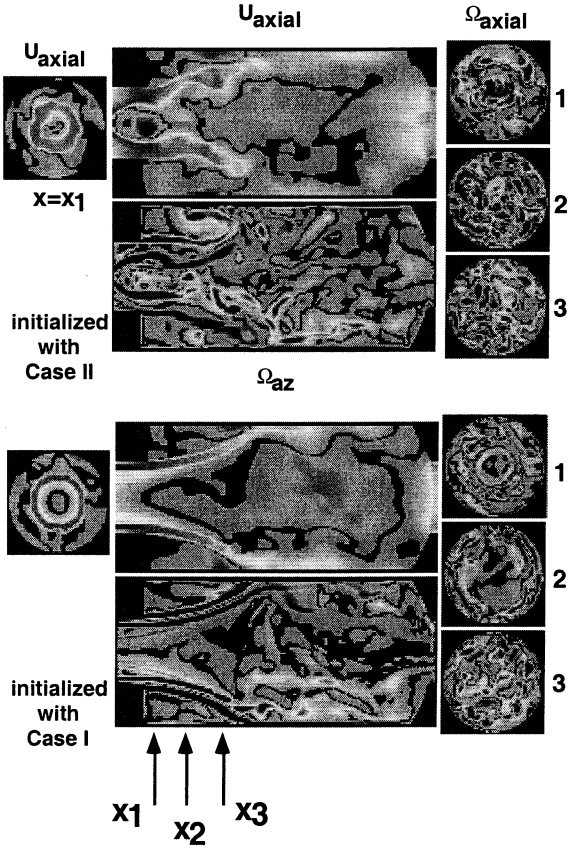

Figure 10. Effects of initial velocity profiles.